

# 1 Investigation of hydrological time series using copulas for detecting

## 2 catchment characteristics and anthropogenic impacts

3 Takayuki Sugimoto<sup>1</sup>, András Bárdossy<sup>1,2</sup> and Geoffrey G. S. Pegram<sup>2</sup>, Johannes Cullmann<sup>3</sup>

4

5 1 Institute for Modelling Hydraulic and Environmental Systems, University of Stuttgart, Stuttgart, Germany

6 2 Civil Engineering Program, University of KwaZulu-Natal, Durban, South Africa

7 3 Federal Institute of Hydrology, Koblenz, Germany

8 **Abstract.** Global climate change can have impacts on characteristics of rainfall-runoff  
9 events and subsequently on the hydrological regime. Meanwhile, the catchment itself  
10 changes due to anthropogenic influences. However, it is not easy to prove the causality  
11 between them in general. In this context, it can be meaningful to detect the temporal  
12 changes of catchments independent from climate change by investigating existing long  
13 term discharge records. For this purpose, a new stochastic system based on copulas for  
14 time series analysis is introduced. While widely used time series models are based on  
15 linear combinations of correlations assuming a Gaussian behavior of variables, a statistical  
16 tool like copula has the advantage to scrutinize the dependence structure of the data in the  
17 uniform domain independent of the marginal.

18 Two measures in the copula domain are introduced herein:

19 1. Copula asymmetry is defined for copulas and calculated for discharges; this measure  
20 describes the non symmetric property of the dependence structure and differs from one  
21 catchment to another due to the intrinsic nature of both runoff and catchment.

22 2. Copula distance is defined as Cramér-von Mises type distance calculated between  
23 two copula densities of different time scales. This measure describes the variability and  
24 interdependency of dependence structures similar to variance and covariance, which can  
25 assist in identifying the catchment changes.

26 These measures are calculated for 100 years of daily discharges for the Rhine rivers.  
27 Comparing the results of copula asymmetry and copula distance between an API  
28 (Antecedent Precipitation Index) and simulated discharge time series by a hydrological  
29 model we can show the interesting signals of systematic modifications along the Rhine  
30 rivers in the last 30 years.

31 **Keywords :** Catchment discharge characteristics, Copula stochastic analysis, API, Model  
32 uncertainty

### 33 1. Introduction

34 In order to understand the water cycle behavior of a region, it is important to determine its characteristics,  
35 but this is difficult to achieve due to the diversity of the system response at different time and space scales.  
36 In particular, temporal variability makes parameter estimation difficult and the assessment of model  
37 uncertainty essential. As a part of the endeavor to grasp the hydrological system, the objective of this  
38 research, assessing the anthropogenic impacts on the catchment characteristic independent of the climate  
39 change is therefore important, yet hard to accomplish.

40 The first possible approach is to statistically test the existence or change of trend in hydrological time  
41 series which can be related to climate changes or anthropogenic impacts. Mann-Kendall's Test was  
42 performed to confirm the existence of a trend in the annual discharge, precipitation and sediment loads, then  
43 ~~and discussed~~ the human intervention and climate impacts based on the available information of the catchments  
44 were discussed (Wu et al., 2012). Pettitt's Method (Pettitt, 1979) can be used to detect the time point of trend  
45 alternation and analyze the impacts based on a double mass curve (Gao et al., 2012) or a hydrological model  
46 (Karlsson et al., 2014). These non-parametric methods for detecting the signal seem, however, not capable  
47 enough of explaining when and how much the system had changed, thus making it still difficult to relate the  
48 change with ~~to~~ human activities.

49 On the other hand, runoff events are initiated by precipitation then modified by the state and physical  
50 features of the catchment. This implies that the integrated information of catchment status might be  
51 retrieved by analyzing the discharge time series itself. Focusing on this property, the attempts can be made  
52 for capturing the temporal dependence structure of runoff by time series models. The classical time series  
53 model, autoregressive integrated moving average (ARIMA), is designed to describe a stationary stochastic  
54 process based on the temporal correlation structure of Gaussian random variables (Box and Jenkins, 1976).  
55 However, the stationarity of the data is not guaranteed in reality, thus a number of alternative approaches  
56 have been suggested. While the application of Fourier Analysis is basically for stationary process, the  
57 analysis using eEmpirical mode decomposition (Huang et al., 1998) is-overcomes the restriction of  
58 stationarity a method designed to overcome the drawbacks of Fourier analysis by allowing the frequency  
59 and local variance of a time series to vary within a component and to separate the signals adaptively by  
60 scale. Autoregressive Conditional Heteroskedasticity (ARCH) models loose the assumption of stationarity  
61 to a certain extent so that variance is not constant, however models the variance in a similar way to  
62 ARIMA. Although the inventions and efforts to overcome the limitation of stationarity are made, it seems  
63 still inadequate to model dynamic changes of hydrological processes with these time series models.

64 Alternatively there is a statistical concept, copulas, which has advantages to model the multivariate  
65 dependence independently from marginals and recently adopted in the field of hydrology. A Copula (Sklar,  
66 1959) is a multivariate probability distribution designed to flexibly model dependence structure in the  
67 uniform (quantile) domain. The use of copulas in hydrology can be found for the assessment of extreme  
68 events by considering flooding as a joint behavior of peak and volume (De Michele and Salvadori, 2003).  
69 Copulas have been applied to describe the spatio-temporal uncertainty of precipitation (Bárdossy and  
70 Pegram, 2009) or the inhomogeneity of groundwater parameters (Bárdossy and Li, 2008). Asymmetry of  
71 dependence in a time series can be tested in the framework of a finite state Markov chain's transition  
72 probability matrix (Sharifdoost et al., 2009). Dissimilarity measures can be defined by means of a copula  
73 modelling the correlation structure of pairs of discharge time series in order to identify the similarity of

74 catchments with the purpose of transferring catchment properties from one to the other (Samaniego et al.,  
75 2010). We aim at utilizing copulas as an alternative to classical time series models and an efficient tool for  
76 time series analysis to overcome these hydrological challenges.

77 The main interest of this study is to precisely assess the human intervention and climate change impacts  
78 on hydrological regime for the strategy of future development in the region. For achieving this goal, 7  
79 daily discharge gauging stations in South-West Germany (Figure 1), which have 100 years daily discharge  
80 records, were chosen and extensively analyzed. The gauging stations Andernach, Kaub, Worms and  
81 Maxau are located in the main stream of the Rhine, while Kalkofen, Cochem and Plochingen are located  
82 on tributaries. For further analysis, daily precipitation and temperature records in the Baden-Württemberg  
83 state of Germany for the last 50 years were obtained from the German Weather Service. Also, 77 discharge  
84 records obtained from the Global Runoff Data Centre in Germany were utilized.

85 What follows is the new aspects introduced in this study: (1) The catchment characteristic is defined based  
86 on copulas and estimated from discharge data. Also the changes of catchment characteristic are  
87 investigated by tracing the temporal change of the ~~these~~ statistics. (2) A method to model systematic changes  
88 of dependence structure with the help of copulas is suggested, then its variability and interrelationship of  
89 the time series are examined. (3) Anthropogenic impacts are assessed by the discharge - precipitation  
90 relation using API and hydrological model with copula based measures.

91 This article is divided into five sections. After the introduction, the basic methodology for applying  
92 copulas to discharge time series is introduced in the second section. Thirdly, the measures of asymmetry in  
93 copulas are defined and estimated for the discharges of the river Rhine and other catchments. The  
94 determination of the temporal change of the asymmetry of the copulas is treated in the third section as well.  
95 In the fourth section two topics are treated: (i) the analysis based on copula distances for the observed  
96 discharges and (ii) the comparison of observed discharge with API (Antecedent Precipitation Index) time  
97 series and simulated discharge time series with a hydrological model. The conclusion is given in the fifth  
98 section.

Field Code Changed

## 99 2. Methodology

100 In this section, the application of copula to time series is articulated after a brief introduction of copulas.  
101 The very basics about copulas are presented here and further information can be obtained from (Joe, 1997)  
102 or (Nelsen, 2006).

### 103 2.1 Basic Methodology

104 In probability theory and statistics, a copula is a multivariate probability distribution for which the  
105 marginal probability distribution of each variable is uniform.

$$106 \quad C : [0,1]^n \rightarrow [0,1] \quad (1)$$

$$107 \quad C(\mathbf{u}^{(i)}) = u_i \quad \text{if } u^{(i)} = (1, \dots, 1, u_i, 1, \dots, 1) \quad (2)$$

108 Any multivariate distribution can be described by a copula and its marginal distributions as was proven by  
109 Sklar's theorem (Sklar, 1959):

$$110 \quad F(\mathbf{x}) = C(F_{x_1}(x_1), \dots, F_{x_n}(x_n)) \quad (3)$$

111 where  $F_{x_i}(x_i)$  represents the i-th marginal distribution of a multivariate random variable  $\mathbf{X}$ . The copula  
112 density can be derived by taking partial derivatives of the copula:

$$113 \quad c(u_1, \dots, u_n) = \frac{\partial^n C(u_1, \dots, u_n)}{\partial u_1 \dots \partial u_n} \quad (4)$$

114 The advantage of using copulas is that the marginal is detached from the multivariate distribution and  
115 the dependence structure can be examined in the uniform compact domain for different types of data.

### 116 2.2 Basic Hypothesis of Temporal Copulas

117 For the application of copulas to time series analysis, a stochastic system should be presumed to be  
118 similar to the case of spatial copulas (Bárdossy and Li, 2008): the random variable at time  $t$  is described as  
119  $Z(t)$  and in general there may exist non-Gaussian dependency among the elements of  $Z(t)$ . Then

stationarity is defined for each subset of times  $t_1, \dots, t_n \subset N$  and time lag  $k$  such that  $\{t_1 + k, \dots, t_n + k\} \subset N$  and for each set of possible values  $z_1, \dots, z_n$ :

$$\begin{aligned} P(Z(t_1) < z_1, \dots, Z(t_n) < z_n) = \\ P(Z(t_1 + k) < z_1, \dots, Z(t_n + k) < z_n) \end{aligned} \quad (5)$$

For the given random function  $Z(t)$ , a set  $S(k)$  containing pairs of ranked values is defined as a function of time lag  $k$  as follows:

$$S(k) = \{(F_z(z(t))), (F_z(z(t+k)))\} \quad (6)$$

Thus, a 2-dimensional autocopula for stochastic time series is a function of time lag  $k$  for the set  $S(k)$  similar to the case of ~~a~~spatial copula (Bárdossy and Li, 2008):

$$C_t(k, u_1, u_2) = P[F_z(Z(t)) < u_1, F_z(Z(t+k)) < u_2] \quad (7)$$

where  $(u_1, u_2) \in S(k)$ . Thus, a 2-dimensional empirical copula density can be constructed based on conditional empirical frequencies on a regular  $g \times g$  grid and kernel density smoothing (Bárdossy, 2006):

$$\begin{aligned} c^*\left(\frac{2i-1}{2g}, \frac{2j-1}{2g}\right) = \frac{g^2}{|S(k)|} \\ \cdot \left| \left\{ (u_1, u_2) \in S(k); \frac{i-1}{g} < u_1 < \frac{i}{g} \text{ and } \frac{j-1}{g} < u_2 < \frac{j}{g} \right\} \right| \end{aligned} \quad (8)$$

where  $|S(k)|$  denotes the cardinality (the number of elements in a set) of set  $S(k)$ .

### 3. Copula Asymmetry in Discharge Time Series

High and low values might have different dependences in general. Measuring the asymmetry of copulas could reveal substantial aspects of time series data, which are not illuminated in the Gaussian approach. Statistics defined on copula shape and calculated from observed discharge time series we believe to be a

new idea. Asymmetry functions are defined on 2-dimensional copulas as a function of time lag  $k$  (Li, 2010):

Asymmetry 1 is defined as:

$$A_1(k) = E[(U_t - 0.5)(U_{t+k} - 0.5)((U_t - 0.5) + (U_{t+k} - 0.5))] \\ = \int_0^1 \int_0^1 (u - 0.5)(v - 0.5)(u + v - 1)c(u, v) du dv$$

~~$$A_1(k) = E[(U_t - 0.5)(U_{t+k} - 0.5)((U_t - 0.5) + (U_{t+k} - 0.5))]$$~~

(9)

Field Code Changed

Asymmetry 2 is defined as:

~~$$A_2(k) = E[(U_t - 0.5)(U_{t+k} - 0.5)((U_t - 0.5) - (U_{t+k} - 0.5))]$$~~

$$A_2(k) = E[-(U_t - 0.5)(U_{t+k} - 0.5)((U_t - 0.5) - (U_{t+k} - 0.5))] \\ = \int_0^1 \int_0^1 -(u - 0.5)(v - 0.5)(u - v)c(u, v) du dv$$

(10)

Field Code Changed

where  $u_t = F_Z(z(t))$ ,  $u_{t+k} = F_Z(z(t+k))$ . Figure 2 shows an idealization of the two asymmetries

between a pair of variables  $U(t)$  and  $U(t+k)$ , showing that the tails of the distributions have a large impact on each type of asymmetry. The measure of asymmetry  $A_1$  compares the dependency between low and high values and  $A_2$  quantifies how much it is not symmetric. For example, in a 2-dimensional copula,  $A_1(k)$  is positive if the probability density is higher in the upper right corner than in the lower left corner.

On the contrary,  $A_1(k)$  is negative if the probability density is higher in the lower left corner than in the upper right.  $A_2(k)$  is the asymmetry for the other diagonal of a 2-dimensional copula.

Figure 3 shows the scatterplot of ranked values of a discharge time series with time lag  $k = 1$  as a sample of an empirical autocopula and its connection with storm water hydrographs relation. Demonstrating (i) the dependence structure is not symmetric especially for  $A_2(k)$ , this figure illustrates (ii) where each pairs of values on hydrograph can be plotted on empirical copula.

For example, sharp rise up of stream flow, which can be characterized as combination of low to high values in empirical copula, is plotted on upper left corner which contributes to the smaller value of asymmetry2 according to the Eq (10)(40). This intrigues the notion that asymmetry might be used for advanced modeling of hydrological time series.

Field Code Changed

161 | ~~Figure 3 shows the scatterplot of ranked values of a discharge time series with time lag  $k = 1$  as a sample~~  
162 | ~~of an empirical autocopula, demonstrating the structure is not symmetric especially for  $A_2(k)$ .~~

### 163 3.1 Asymmetry and catchment characteristics

164 | Asymmetries can be considered as statistics calculated from the observed discharge time series and leads  
165 | to have an important assumption: ‘assymetry2 is related to catchment characteristics’. This idea will be  
166 | exclusively~~intensively~~ discussed ~~and~~ demonstrated in this section. Figure 5 (upper left) shows part of the  
167 | hydrographs of 7 gauging stations in southwest Germany.

168 | First, an important ~~and obvious~~ natural property of discharge seen in this figure is that the duration of  
169 | high flow and low flow periods is not symmetric: Flood events, which are initiated by rainfall or snowmelt,  
170 | do not continue for a long time because the duration of runoff to rivers is comparatively short. On the other  
171 | hand, discharge keeps decreasing and stays low for no rain periods. This means that, if two consecutive  
172 | values in a time series are chosen for small time lag  $k$ , these two values are likely to be less correlated for  
173 | high values but more correlated for low values, which leads to negative value of  $A_1(k)$ . This asymmetry  
174 | can be related to the intrinsic temporal distribution of precipitation.

175 | Second, the increase and decrease of discharge is not symmetric: Soon after the rainfall, the river flow  
176 | rises sharply. Once the rain stops and peak discharge is observed, then the water level starts to decrease,  
177 | typically more slowly on the recession than the rising limb of the hydrograph, which leads to negative  
178 | values of  $A_2(k)$  for small time lags  $k$ . This asymmetry can be related to the characteristics of the runoff  
179 | and catchment.

180 | The change of  $A_2(k)$  with time lag  $k$  [days] is now discussed. The point is that these statistics for small  
181 | time lags  $k$  can be more related to the catchment and rainfall characteristics of the region, while asymmetry  
182 | for larger time lags  $k$  can capture the inter-seasonal characteristic of the climate in the region.

Field Code Changed

In order to reduce such seasonal impacts in hydrological time series deseasonalization measure can be applied, for example, especially for daily stream flow (Grimaldi, 2004). Following this method, all the time series are normalized in this study.

~~In order to reduce this seasonal impact, normalization was adopted for the time series similar to z score in the following way. First, the annual cycle of the mean  $\mu_i$  on the i-th calendar day is calculated as expectation of random variable  $X_i$ . Then, the annual cycle of the mean  $\mu_i^*$  is calculated as smoothed version of  $\mu_i$  by linearly weighting the neighboring values along  $i$  and summing up them. The annual cycle of standard deviation  $\sigma_i^*$  can be obtained in the same way. Then the normalized time series are defined by dividing the original time series  $Z(t)$  by  $\sigma_i^*$  after subtracting  $\mu_i^*$  as follow~~

$$Z_{norm}(t) = \frac{Z(t) - \mu_i^*}{\sigma_i^*} \quad (11)$$

~~and smoothed by linear weighting~~

$$\begin{aligned} \mu_{t|365} &= E[X_{t|365}] \\ \mu_{t|365}^* &= \frac{1}{2N} \sum_{i=0}^{N/2} \left( \frac{1}{2} - \frac{i}{N} \right) (\mu_{t+i|365} + \mu_{t-i|365}) \end{aligned} \quad (11)$$

~~where  $t|365$  is  $t \pmod{365}$  and represents calendar day at time  $t$  [day].  $X_i$  denotes the random variable of discharge,  $\mu_i$  denotes mean and  $\mu_i^*$  denotes mean after smoothing on calendar day  $i$  respectively. After subtraction of the annual mean from the original time series  $Z(t)$ , the annual cycle of standard deviation is defined.~~

$$\begin{aligned} \sigma_{t|365} &= E \left[ \sqrt{(X_{t|365} - \mu_{t|365})^2} \right] \\ \sigma_{t|365}^* &= \frac{1}{2N} \sum_{i=0}^{N/2} \left( \frac{1}{2} - \frac{i}{N} \right) (\sigma_{t+i|365} + \sigma_{t-i|365}) \end{aligned} \quad (12)$$

~~Figure 4 shows the annual cycles after smoothing described by equations (11) and (12). By subtracting the annual mean cycle and dividing by annual standard deviation cycle, the normalized time series is defined.~~

Formatted: Lowered by 15 pt

Field Code Changed

Formatted: Text

$$Z_{norm}(t) = \frac{Z(t) - \mu_{t|365}^*}{\sqrt{\sigma_{t|365}^*}} \quad (13)$$

Figure 5 (upper right) shows part of normalized discharge time series from the 7 gauging stations. It should be noted that the process still appears to be non-Gaussian after this transformation and the seasonality for small time lags  $k$  might not be fully eliminated. Figure 5 (bottom left and bottom right) shows the variation of asymmetry functions for 7 discharge time series corresponding to time lag  $k$  similar to the correlograms in addition to the confidence interval of Gaussian process.

The confidence intervals in the figures are gained by calculating  $A_2(k)$  for 100 realizations of stationary Gaussian process which are fitted to the observed discharge of Andernach. The result shows that the process is clearly different from Gaussian and the influence of asymmetry is significantly large.

It can be seen that the variation of  $A_2(k)$  of discharge without normalization (Figure 5 bottom left) has a larger impact of seasonality for bigger  $k$  ( $k > 40$ ), while its impacts are mitigated after the normalization (Figure 5 bottom right). Furthermore, as a consequence of normalization, a sharp drop down of  $A_2(k)$  for small time lags  $k$  emerged which might be regarded as a catchment indicator. Therefore, the selected/critical properties for small time lags  $k$  is formulated by (i) taking the minimum value of  $A_2(k)$  for the time lag  $k < 50$  and (ii) the lag  $k$  at the minimum of asymmetry2:

$$A_{2,\min} = \min_{k < 50} A_2(k) \quad (12)$$

$$L_{2,\min} = \min_{0 < k < 50} \{k; A_2(k) = A_{2,\min}\} \quad (13)$$

The question is whether they are really related to catchment characteristics. Now, these statistics estimated for 77 discharge data recorded at the gauging stations in Germany are compared with the catchment area as one of the simplest possible indicators of the catchment as shown in Figure 6:  $A_{2,\min}$  - area (Figure 6 top) shows a more clear linear relation than  $L_{2,\min}$  - area (Figure 6 middle) while the

223 dispersions  $A_{2,\min}$  and  $L_{2,\min}$  for the smaller catchments are big for both cases. The correlation between  
 224  $A_{2,\min}$  and  $L_{2,\min}$  (Figure 6 bottom) is slightly positive.

225 This demonstrates that the information extracted from discharge is related to the basic information of its  
 226 catchment to a certain extent. Since the principal objective is to assess anthropogenic impacts, the idea  
 227 introduced now is to use this measure for evaluating the catchment change by calculating chronological  
 228 changes of  $A_{2,\min}$ .

### 229 3.2 Time Series Analysis with Asymmetry

230 Temporal change of asymmetry  $A_2(k, t)$  is defined on the set representing a moving time window of  
 231 size  $w$ .

$$232 \quad S^*(k, t) = \left\{ (F_Z(z(a))), (F_Z(z(a+k))); t - \frac{w}{2} < a < t + \frac{w}{2} \right\} \quad (14)$$

$$233 \quad \begin{aligned} A_2(k, t) &= E[-(U_t - 0.5)(U_{t+k} - 0.5)((U_t - 0.5) - (U_{t+k} - 0.5))] \\ &= \int_0^1 \int_0^1 -(u_t - 0.5)(u_{t+k} - 0.5)(u_t - u_{t+k}) c(u_t, u_{t+k}) du_t du_{t+k} \end{aligned} \quad (15)$$

235 where  $u_t \in U_t, u_{t+k} \in U_{t+k}, (u_t, u_{t+k}) \in S^*(k, t)$ . Then the minimum of asymmetry2 and lag  $k$  at the  
 236 minimum of asymmetry2 at time  $t$  are given by

$$237 \quad A_{2,\min}(t) = \min_{k < 30} A_2(k, t) \quad (16)$$

$$238 \quad L_{2,\min}(t) = \min_{0 < k < 30} \{k; A_2(k, t) = A_{2,\min}(t)\} \quad (17)$$

239 Figure 7 shows the temporal changes of  $A_{2,\min}(t)$  with window size  $w = 3000$  [days] for 7 gauging  
 240 stations in southwest Germany in addition to the confidence interval calculated for 100 times independently  
 241 generated Gaussian process.

242 The comparison of  $A_{2,\min}(t)$  from observed discharges with  $A_{2,\min}(t)$  from a Gaussian process exhibits  
 243 (i) the influence of asymmetry in discharge is significantly large as it was seen in Figure 5. (ii) The  
 244 fluctuations of  $A_{2,\min}(t)$  of 7 observed discharge time series appear to be bigger than the one calculated for  
 245 a realization of a Gaussian process. (iii)  $A_{2,\min}(t)$  of these 7 discharge records shows a similar trend: there  
 246 are big drop-downs around 1945 and after 1980 for all the discharges.

247 However, it cannot be ascertained whether this is caused by the simultaneous change of the catchments,  
 248 the long term meteorological behavior in the region or just randomness in the stationary process. To  
 249 overcome this, temporal behavior of discharge and temperature were first checked by calculating the mean,  
 250 the standard deviation and the minimum at time  $t$  defined by

$$\begin{aligned}
 \text{Mean}(t) &= \frac{1}{w} \int_{t-w/2}^{t+w/2} z(a) da \\
 \text{Std}(t) &= \sqrt{\text{Var}(t)} = \frac{1}{w} \left( \int_{t-w/2}^{t+w/2} (z(a) - E[Z(t)])^2 da \right)^{\frac{1}{2}} \\
 \text{Min}(t) &= \min \left\{ Z(a); t - \frac{w}{2} < a < t + \frac{w}{2} \right\}
 \end{aligned} \tag{18}$$

252 where  $w$  is the size of time window. Figure 8 shows moving average and moving standard deviation of  
 253 discharge records with windows size  $w = 3000$  [days], but it is hard to say whether the behavior around  
 254 1945 and after 1980 is unusual. Figure 9 shows mean and minimum of temperature in the time window  
 255 with size 365 [days] which correspond to annual mean and minimum. Roughly speaking, there are certain  
 256 cold periods around 1940, 1955 and 1985, which might influence the snow accumulation and melting in  
 257 the region, but the relation with asymmetry2 is rather obscure.

258 What seems to be a useful outcome from the above exploratory analysis is that (i) the behavior of  
 259 asymmetry2 is different from catchment to catchment showing a statistical relation with the catchment area  
 260 and (ii) temporal behaviors of asymmetry2 of 7 discharges time series are dependent on each other, which  
 261 implies the existence of a background mechanism common to the region.

#### 262 4. Analysis of hydrological time series with Copula Distance

As an alternative to copula asymmetry, which emphasizes the behavior on the corner of copulas, copula distance is here suggested so that the characteristic behavior can be captured in the entire domain of the copula. Calculating this for each time step for different time series and comparing them hopefully exhibits the changes of dependence structure and therefore the catchment change.

#### 4.1 Introduction of Copula Distance

The basic idea behind the copula distance is to apply the Cramér-von Mises type distance

$$D = \int_0^1 \int_0^1 (C^*(u_1, u_2) - C(u_1, u_2))^2 du_1 du_2 \quad (19)$$

, which by design measures the goodness of fit between two distribution functions, to two copulas. This type of distance was tested to measure the difference between empirical and theoretical copula in the bootstrap framework for the evaluation of spatial dependence of ground water quality (Bárdossy, 2006). For the analysis of time series data, it still needs to be carefully thought out how (and which) copulas should be chosen.

##### 4.1.1 Introduction of Copula Distance to single time series

In order to apply the concept of copula distance to time series, the adoption of two copulas in different time scales is considered. An empirical copula can be obtained from an entire time series which contains the averaged information of all the time points (*global copula*). Another empirical copula can be obtained for a certain window of width  $w$  at time step  $t$  (*local copula*). In order to make the concept clear, two sets containing pairs of ranked values with different time scales are specified.

$$S_{global}(k) = \{(F_Z(z(t))), (F_Z(z(t+k)))\}; t_1 < t < t_n\} \quad (20)$$

$$S_{local}(k, t) = \{(F_Z(z(a))), (F_Z(z(a+k)))\}; t - \frac{w}{2} < a < t + \frac{w}{2}\} \quad (21)$$

$S_{local}(k, t)$  can be interpreted as a moving time window where the reference time  $t$  is set to the middle of the window of size  $w$ , while  $S_{global}(k)$  represents a set of the entire time series. *Global copula* and *local*

285 | *copula* are the empirical autocopula densities defined on these sets based on Equation ~~(8)~~(8), there denoted  
 286 by  $c_{global}^*(\mathbf{u})$  and  $c_{local}^*(\mathbf{u}, t, w)$  respectively for the n-dimensional case. In this analysis, 3000 [days] for the  
 287 time window  $w$  and a 3-dimensional copula separated with 1 day gap between each variable are employed.  
 288 This means

$$289 \quad \mathbf{u} = (u_0, u_1, u_2) \quad (22)$$

290 where  $u_0 = F_z(Z(t))$ ,  $u_1 = F_z(Z(t+1))$ ,  $u_2 = F_z(Z(t+2))$ , then the deviation of local copula from global  
 291 copula is defined by

$$292 \quad \Delta c(\mathbf{u}, t) = c_{local}^*(\mathbf{u}, t) - c_{global}^*(\mathbf{u}) \quad (23)$$

293 For the first approach, the comparison of dependence structures between entire and local time series is  
 294 done for detecting unusual dependence structures. To this end, *copula distance type1* is defined by taking  
 295 the copula distance between global and local copula at each time step  $t$

$$296 \quad \begin{aligned} D_1(c, t) &= \int_0^1 \dots \int_0^1 (c_{global}^*(\mathbf{u}) - c_{local}^*(\mathbf{u}, t))^2 du_1 \dots du_n \\ &= \int_0^1 \dots \int_0^1 \Delta c(\mathbf{u}, t)^2 du_1 \dots du_n \end{aligned} \quad (24)$$

297 Second, *copula distance type 2* is introduced for indicating the point at which the structure of copulas starts  
 298 to change. For this method, the distance between two local copulas is calculated from the 2 time intervals

$$299 \quad D_2(c, t) = \int_0^1 \dots \int_0^1 \left( c_{local}^*\left(\mathbf{u}, t - \frac{w}{2}\right) - c_{local}^*\left(\mathbf{u}, t + \frac{w}{2}\right) \right)^2 du_1 \dots du_n \quad (25)$$

300 Note that reference time is set to the middle of both time windows and shifted for  $w/2$  [days] from each  
 301 other where the size of the time windows is  $w$ . Therefore, there is no overlapping part between the two  
 302 time intervals of these two local copulas. For the comparison, the moving variance is introduced as  
 303 follows:

$$304 \quad \begin{aligned} E[Z(t)] &= \frac{1}{w} \int_{t-w/2}^{t+w/2} z(a) da \\ Var(t) &= \frac{1}{w} \int_{t-w/2}^{t+w/2} (z(a) - E[Z(t)])^2 da \end{aligned} \quad (26)$$

Field Code Changed

Figure 10 shows the result of  $D_1(t)$ ,  $D_2(t)$  and  $Var(t)$  in the moving time window for the normalized discharge time series between 1940 to 2000 at 4 gauging stations located in the main stream of the Rhine (Andernach, Maxau ) and its two different tributaries (Cochem, Plochingen) in addition to the 90 % confidence intervals calculated for the Gaussian process fitted to the discharge data of Andernach.

First of all, the values of these 2 measures at Cochem and Plochingen are bigger and more fluctuating in general. The reason could be that their catchments and discharges are smaller, thus more sensitive to changes. Second, it can be said that the dependence structure is not homogeneous over the time period, but the local copula clearly deviates from the global copula for certain time periods. For example, the value of  $D_1(t)$  is remarkably big around 1947, 1982 and 2000 for all the 4 discharge records (pointed by white arrows).  $D_2(t)$  is also big around 1977 for all the data. This signal of  $D_2(t)$  implies that a simultaneous change of runoff behavior occurred in this region at 1977, which can be related to the high value of  $D_1(t)$  at 1982.  $Var(t)$  is also changing, but the direct relation with  $D_1(t)$  and  $D_2(t)$  is hard to recognize. Also the confidence interval of the Gaussian process is clearly smaller than the observed one. This indicates the copula distances of the stationary process are small while the nature process is non-stationary and its dependence structure is more varying.

For copula distance type1, the global copula can be considered as an average state of the copula, while the local copula can be regarded as a realization of a possible state of a copula at time step  $t$ . This concept can be comparable to variance and leads to a new measure, *copula variance*, which is the summation of copula distances between global and local copula over the time.

$$Var_{cop}(c) = \frac{1}{t_n - t_1} \int_{t_1}^{t_n} D_1(c, t) dt \quad (27)$$

Field Code Changed

[Table 1](#) shows the variance and copula variance calculated for the 4 discharge data. The result demonstrates that copula variance of the time series can be higher, even if the conventional variance is lower for example in case of Maxau.

#### 328 4.1.2 Copula Distance for two time series

329 In the previous section, copula variance was defined as a measure of the variability characteristic of the  
 330 copula itself. Here, it is examined whether covariance can be defined for two copula densities  $c_1$  and  $c_2$   
 331 from two time series as *copula distance type3*, which shows whether the variability characteristic of  
 332 copulas is related to each other.

$$333 D_3(c_1, c_2, t) = \int_0^1 \dots \int_0^1 \Delta c_1(\mathbf{u}, t) \Delta c_2(\mathbf{u}, t) du_1 \dots du_n \quad (28)$$

334 where

$$335 \begin{aligned} \Delta c_1(\mathbf{u}, t) &= c_{1,local}^*(\mathbf{u}, t) - c_{1,global}^*(\mathbf{u}) \\ \Delta c_2(\mathbf{u}, t) &= c_{2,local}^*(\mathbf{u}, t) - c_{2,global}^*(\mathbf{u}) \end{aligned} \quad (29)$$

336 By its definition, the value of  $D_3(t)$  can be related to  $D_1(t)$  because  $D_3(t)$  compares the deviation of local  
 337 copulas from global copulas in a similar way to  $D_1(t)$  in Equation (26). In order to reduce the influence of  
 338  $D_1(t)$  on  $D_3(t)$ , *copula distance type4* is introduced as a normalized measure bounded between -1 and 1  
 339 analogous to correlation.

$$340 D_4(c_1, c_2, t) = \frac{D_3(c_1, c_2, t)}{\sqrt{D_1(c_1, t)} \cdot \sqrt{D_1(c_2, t)}} \quad (30)$$

341 where  $|D_4(c_1, c_2, t)| \leq 1$ . For comparison, covariance and correlation in a moving window are introduced for  
 342 two random variables  $Z_1(t)$  and  $Z_2(t)$  as follows:

$$343 Cov(t) = \int_{t-w/2}^{t+w/2} (z_1(a) - E[Z_1(t)])(z_2(a) - E[Z_2(t)]) da \quad (31)$$

$$344 Cor(t) = \frac{Cov(t)}{\sqrt{Var(Z_1(t))} \cdot \sqrt{Var(Z_2(t))}} \quad (32)$$

345 Figure 11 shows the copula distance between two time series  $D_3(t)$  and  $D_4(t)$  in addition to the  
 346 covariance and correlation in moving time window.

First, it can be said that the behavior of covariance and correlation in a moving window are different from  $D_3(t)$  and  $D_4(t)$ . This implies these two copula based statistics exhibit different properties of the time series from ordinary statistics. Second,  $D_3(t)$  shows high values around 1947, 1982 and 2000, which is same to the case of  $D_1(t)$  in Figure 10. This indicates that unusual states of copulas in 4 discharge time series can be related to each other. Third,  $D_4(t)$  is in general high except for the period around 1970 and 1990. This means, the temporal behavior of dependence structures for these 4 discharges are actually similar except for these periods even if  $D_1(t)$  and  $D_3(t)$  are small.

Copula covariance and copula correlation can be defined similar to copula variance in order to quantify the overall behavior of two time series.

$$Cov_{cop}(c_1, c_2) = \frac{1}{t_2 - t_1} \int_{t_1}^{t_2} D_3(t) dt \quad (33)$$

$$Cor_{cop}(c_1, c_2) = \frac{Cov_{cop}(c_1, c_2)}{\sqrt{Var_{cop}(c_1)} \cdot \sqrt{Var_{cop}(c_2)}} \quad (34)$$

where  $|Cor_{cop}(c_1, c_2)| \leq 1$  and its derivation can be found in appendix A. In [Table 2](#), these copula based statistics are compared with ordinary statistics. For example, Cochem and Plochingen are located remotely in different tributaries, thus covariance and correlation are lower than the others, but copula covariance and copula correlation are not the lowest.

The measures using copula distance are different from the conventional statistics. This behavior can be explained by the fact that the autocopula has more substantial information about temporal dependence structure than the autocorrelation. Using these measures might enable us to take advantage of a different way of seeing the dependence between time series.

What is new in the analysis of this section is that (i) measures based on copula distance show the different properties of time series in comparison to conventional statistics and (ii) there are significant signals of copula distances for certain time periods in common to all the discharge data.

## 369 4.2 Copula based Stochastic Analysis with API and Hydrological Model

370 The difficulty of analyzing discharge time series in order to detect catchment change is that it is not clear  
371 whether the temporal change of stochastic information is caused by catchment change or merely by  
372 random behavior of precipitation. To gain an understanding of this process, we attempted to eliminate the  
373 influence of precipitation using, first, API (antecedent precipitation index) for comparison with discharge ,  
374 second, using a hydrological model with the parameter sets calibrated and fixed for the entire simulation  
375 time period.

### 376 4.2.1 Copula Distance Analysis with API

377 An API (Antecedent Precipitation Index) time series, which is generated from observed precipitation  
378 time series and behaves similarly to discharge, is used instead of precipitation.

$$379 \quad API(t+1) = \alpha API(t) + P(t+1) \quad (35)$$

380 where  $P(t)$  is daily precipitation [mm/day],  $API(t)$  is time series of API [mm/day] and  $\alpha = 0.85$  was  
381 chosen. The assumption for this method is that the API time series has the stochastic information purely  
382 originated from the precipitation, while observed discharge is supposed to be influenced by both  
383 catchments and precipitations. If the stochastic information derived from these two data sets is the same,  
384 this indicates that the stochastic turbulence is originating from precipitation; otherwise the change is from  
385 the catchment.

386 For this investigation, precipitation data was carefully chosen for 4 regions (northwest, northeast,  
387 southwest and central) of Baden-Württemberg (Germany) so that they have several almost continuous  
388 daily records between 1935 and 2005. Figure 12 shows the locations of measuring stations. The  
389 precipitation time series were aggregated into one for each region by taking daily average, then 4 API time  
390 series was calculated in total by Equation ~~(35)~~(35). Figure 13 shows the result of copula distances  
391  $D_1(t), D_2(t)$  and moving average  $Var(t)$  for API time series with the 90% confidence intervals of the

Field Code Changed

Field Code Changed

Field Code Changed

392 Gaussian process. Figure 14 shows the result of copula distances  $D_3(t)$ ,  $D_4(t)$  and moving covariance and  
393 correlation for API time series.

394 What can be recognized first in this Figure 13 is that the magnitudes of  $D_1(t)$  and  $D_2(t)$  are smaller than  
395 the case of discharge. This is considered to happen as a result of aggregation of precipitation time series  
396 and adoption of API, but some signals can be still identified:  $D_1(t)$  around 1947 and 2000 is high, but not  
397 much for 1982. The signal of  $D_2(t)$  which was detected around 1977 in Figure 11 does not seem to exist  
398 for API. This can be even more clear for  $D_3(t)$  in Figure 14 that there is no common change of the  
399 dependence structure around 1982 in API time series. This is interesting due to the following implications:

400 (i) the noises of  $D_1(t)$  in ~~Figure 13~~ **Figure 13** were reduced and signals in common were amplified (ii) the  
401 unusual state of copula around 1982 is not caused not by precipitation, but could be caused by the  
402 catchment change.

403 For further verification, copula distance type3 and type4 between discharge and API time series were  
404 calculated as shown in Figure 15. This result also shows there is no clear relation between API and  
405 discharge time series around 1982.

406 **4.2.2 Copula based analysis with a hydrological model**

407 API time series were calculated by spatially aggregating several daily precipitations records in each region  
408 of Baden-Württemberg state. In this section, simulated discharges time series are generated by a  
409 conceptual hydrological model, HBV (Bergström 1976 ; Bergström, Singh, and others 1995) ,which takes  
410 daily precipitations and temperatures records as input and simulates discharges for smaller catchments as  
411 more robust sample of discharge to compare with observed discharge in order to check if differences might  
412 occur due to the method.

413 Thus the idea behind this methodology is similar to the case of API: A hydrological model with the  
414 parameters fixed for the entire time period represents the catchment not influenced by anthropogenic

Field Code Changed

Field Code Changed

Field Code Changed

Field Code Changed

Field Code Changed

Field Code Changed

415 impacts. Then, the discharges simulated by this model should not reflect on the catchment change, while  
416 observed discharge is assumed to be influenced by both catchment and precipitation.

417 For the study area, Upper Neckar Catchment was chosen as drawn in Figure 12. One parameter set  
418 needed for this model constitutes of 13 parameters which are calibrated based on the Nash–Sutcliffe model  
419 efficiency coefficient using the simulated annealing algorithm for the period between 1960 and 2000. Then,  
420 30 parameter sets are independently calibrated in total and, subsequently, 30 simulated discharges time  
421 series are generated to compare with one observed discharge.

422 Figure 16 shows the result of copula based analysis calculated for single time series  
423  $(D_1(t), D_2(t), A_{2,min}(t))$ . It can be seen that  $A_{2,min}(t)$  in Figure 16 (top) that (i) fluctuations of  $A_{2,min}(t)$   
424 of observed and simulated discharge are locally identical. This implies that the short term behavior of  
425  $A_{2,min}(t)$  is originated from the temporal behavior of precipitation but (ii) there exists a change of trend  
426 around 1976:  $A_{2,min}(t)$  of observed discharge is slightly bigger than simulated before 1976, while  
427  $A_{2,min}(t)$  of observed discharge clearly undershoot the simulated ones of after 1976. This change of trend  
428 was also seen in the previous analyses ( $D_2(t)$  in Figure 10). Furthermore,  $D_1(t)$  in Figure 16 (middle) is  
429 high before 1976 which indicates the state of the copula is different from the rest, while the result of  
430 simulated discharges does not show such tendency.  $D_2(t)$  in Figure 16 (bottom) indicates the change of  
431 dependence structure happened around 1970 and 1977. These results using the HBV model indicate the  
432 change of the dependence structure detected using copulas around 1976 is not caused by the random  
433 behavior of precipitation, but by the behavior of the catchment itself.

434 The fact and the notion obtained in this section is that (i) both results from API and HBV based on  
435 copula measures indicate that the catchment changed around 1976 and (ii), by comparing the simulated  
436 discharge with observed discharge, the origin of the change of stochastically information can be assessed.

437

Field Code Changed

Field Code Changed

Field Code Changed

Field Code Changed

Field Code Changed

Field Code Changed

## 438 Conclusion

439 In this paper the application of copulas for hydrological time series data is newly explored for the  
440 detection of catchment characteristics and their temporal changes.

441 1. A Copula based measure, asymmetry, was defined and newly applied for the identification of  
442 catchment characteristics. Indeed, it ~~was is presumed presented~~ that asymmetry2 ~~is can be~~ related to the  
443 runoff characteristics.

444 2. The relation between the minimum of asymmetry2 and catchment characteristics was tested for 77  
445 discharge records. Asymmetry2 has a certain relation especially with bigger catchments and this  
446 strengthens the notion that asymmetry2 can be used as a statistic to explain the catchment state.

447 3. Temporal change of asymmetry2 was calculated as an index of the catchment state and demonstrated  
448 it keeps changing coincidentally with time. However, it is difficult to explain the causality, at least, by long  
449 term behavior of discharge and temperature time series.

450 4. A method based on copula distance was examined for the investigation of temporal behavior of  
451 hydrological time series. This measure can detect the time period where dependence structure is unusual  
452 and its interdependency. Clear signals were detected that the dependence structure is unusual for a certain  
453 time period and the signal was not found by investigating the time series with variance, covariance or  
454 correlation.

455 5. API time series were generated for each region in the Baden-Württemberg state and simulated  
456 discharge time series were generated using the HBV model for the Upper Neckar Catchment. These are the  
457 data not influenced by the catchment change, thus compared with observed discharge to assess the  
458 anthropogenic impacts. The results showed that there was a signal detected only in the observed discharge  
459 around 1982, but not in the API or simulated time series, which implies the anthropogenic impacts on the  
460 catchment. Also it was shown in the results of copula asymmetry that ~~the difference of  $A_{2,\min}(t)$  between~~  
461 ~~observed and simulated discharge was not constant, but~~ the trend clearly changed around 1976.

462 The results of copula based analysis of hydrological time series seem to support the assumption that the  
463 catchment had started to change around 1976 and stayed unusual until 1990. These changes could  
464 correspond to the construction of flood retention basins started around 1982 (Lammersen et al., 2002) and  
465 ecological flooding strategy, which let small floods to happen for the rehabilitation of ecological systems  
466 in the floodplain, introduced in the Upper Rhine since 1989 (Siepe, 2006).

467 Copulas can be an alternative method to analyze the hydrological time series data by focusing on the  
468 dependence structure, but further applications and theoretical developments are expected in this frame  
469 work. The copula based techniques introduced here for estimating catchment change can be related to the  
470 potential model uncertainty.—Empirical autocopula is a more data driven approach which retains more  
471 information than the copulas estimated with parametric methods, but it is also numerically demanding. The  
472 effective way to analyze time series and build up a time series model based on copula can be further  
473 explored.

474

Field Code Changed

Field Code Changed

Field Code Changed

475  
476  
477

478 **Appendix A**

479 Suppose that a random variable at time  $t$  is denoted as  $X(t)$  and  $c_X(\mathbf{u}, t)$  is an autocopula obtained from  
 480  $X(t)$ . Assuming  $c_{X,mean}(\mathbf{u})$  as an average state of  $c_X(\mathbf{u}, t)$ , deviation of copula  $\Delta c_X(\mathbf{u}, t)$  at time  $t$  is  
 481 defined by

$$482 \quad \Delta c_X(\mathbf{u}, t) = c_X(\mathbf{u}, t) - c_{X,mean}(\mathbf{u}) \quad (A1)$$

483 For the empirical case,  $c_X(\mathbf{u}, t)$  and  $c_{X,mean}(\mathbf{u})$  can be regarded as local copula and global copula  
 484 respectively similar to Equation (29)(29). Since global and local copula are empirical copula density as  
 485 defined in equation (8)(8),  $\Delta c_X(\mathbf{u}, t)$  can be regarded as a vector of values on finite number of grids:

$$486 \quad \Delta \mathbf{c}_X(t) = (\Delta c_{X,1}(t), \Delta c_{X,2}(t), \dots, \Delta c_{X,i}(t), \dots, \Delta c_{X,N}(t)) \quad (A2)$$

487 where  $\Delta c_{X,i}(t)$  denotes the value of copula density at  $i$ -th grid and  $N$  is the number of grids. From  
 488 Cauchy-Schwarz inequality

$$489 \quad \|\Delta \mathbf{c}_X(t)\| \|\Delta \mathbf{c}_Y(t)\| \geq \left| \langle \Delta \mathbf{c}_X(t), \Delta \mathbf{c}_Y(t) \rangle \right|^2 \quad (A3)$$

490 where  $\|\Delta \mathbf{c}_X(t)\|$  is norm and  $\langle \Delta \mathbf{c}_X(t), \Delta \mathbf{c}_Y(t) \rangle$  is inner product of vector  $\Delta \mathbf{c}_X(t)$  and  $\Delta \mathbf{c}_Y(t)$ . Then

$$491 \quad \begin{aligned} \|\Delta \mathbf{c}_X(t)\| &= \sum_{i=1}^N \Delta c_{X,i}(t)^2 \\ &= \int_0^1 \dots \int_0^1 (\Delta c_X(\mathbf{u}, t))^2 du_1 \dots du_n = D_1(c_X, t) \end{aligned} \quad (A4)$$

$$492 \quad \begin{aligned} &\left| \langle \Delta \mathbf{c}_X(t), \Delta \mathbf{c}_Y(t) \rangle \right|^2 \\ &= \langle \Delta \mathbf{c}_X(t), \Delta \mathbf{c}_Y(t) \rangle = \sum_{i=1}^N \Delta c_{X,i}(t) \cdot \Delta c_{Y,i}(t) \\ &= \int_0^1 \dots \int_0^1 \Delta c_X(\mathbf{u}, t) \Delta c_Y(\mathbf{u}, t) du_1 \dots du_n = D_3(c_X, c_Y, t) \end{aligned} \quad (A5)$$

$$493 \quad \frac{\left| \langle \Delta \mathbf{c}_X(t), \Delta \mathbf{c}_Y(t) \rangle \right|^2}{\|\Delta \mathbf{c}_X(t)\| \|\Delta \mathbf{c}_Y(t)\|} = \frac{D_3(c_X, c_Y, t)^2}{D_1(c_X, t) \cdot D_1(c_Y, t)} = D_4(c_X, c_Y, t)^2 \leq 1 \quad (A6)$$

Therefore  $|D_4(c_X, c_Y, t)| \leq 1$  in Equation (30)(39). Above inequality is valid for certain time point  $t$  and summing up (A6) for all the time steps  $t$  leads to

$$\sum_{t=1}^T (\|\Delta \mathbf{c}_X(t)\| \cdot \|\Delta \mathbf{c}_Y(t)\|) \geq \sum_{t=1}^T |\langle \Delta \mathbf{c}_X(t), \Delta \mathbf{c}_Y(t) \rangle| \quad (\text{A7})$$

where  $T$  is the number of time steps.  $\|\Delta \mathbf{c}_X(t)\|$  is a norm and can be denoted for simplicity as

$x_t = \|\Delta \mathbf{c}_X(t)\|$ . Then

$$\sum_{t=1}^T (\|\Delta \mathbf{c}_X(t)\| \|\Delta \mathbf{c}_Y(t)\|) = \langle \mathbf{x}, \mathbf{y} \rangle \quad (\text{A8})$$

where  $\mathbf{x} = (x_1, x_2, \dots, x_T)$ ,  $\mathbf{y} = (y_1, y_2, \dots, y_T)$  for  $t = 1 \dots T$ . Again from Cauchy-Schwarz inequality

$$|\langle \mathbf{x}, \mathbf{y} \rangle|^2 \leq \|\mathbf{x}\| \|\mathbf{y}\| \quad (\text{A9})$$

where

$$\begin{aligned} \|\mathbf{x}\| \cdot \|\mathbf{y}\| &= \sum_{t=1}^T x_t^2 \cdot \sum_{t=1}^T y_t^2 = \sum_{t=1}^T \|\Delta \mathbf{c}_X(t)\|^2 \cdot \sum_{t=1}^T \|\Delta \mathbf{c}_Y(t)\|^2 \\ &= \sum_{t=1}^T D_1(c_X, t)^2 \cdot \sum_{t=1}^T D_1(c_Y, t)^2 = T^2 \cdot \text{Var}_{cop}(c_X) \cdot \text{Var}_{cop}(c_Y) \end{aligned} \quad (\text{A10})$$

$$\begin{aligned} \langle \mathbf{x}, \mathbf{y} \rangle &= \sum_{t=1}^T (x_t \cdot y_t) = \sum_{t=1}^T (\|\Delta \mathbf{c}_X(t)\| \cdot \|\Delta \mathbf{c}_Y(t)\|) \geq \sum_{t=1}^T |\langle \Delta \mathbf{c}_X(t), \Delta \mathbf{c}_Y(t) \rangle| \\ &= \sum_{t=1}^T D_{3,XY}(t) = T \cdot \text{Cov}_{cop}(c_X, c_Y) \end{aligned} \quad (\text{A11})$$

Then  $|\langle \mathbf{x}, \mathbf{y} \rangle|^2 \leq \|\mathbf{x}\| \|\mathbf{y}\|$  indicates

$$\begin{aligned} |\text{Cov}_{cop}(c_X, c_Y)|^2 &\leq \text{Var}_{cop}(c_X) \text{Var}_{cop}(c_Y) \\ |\text{Cor}_{cop}| &= \frac{\text{Cov}_{cop}(c_X, c_Y)}{\sqrt{\text{Var}_{cop}(c_X)} \cdot \sqrt{\text{Var}_{cop}(c_Y)}} \leq 1 \end{aligned} \quad (\text{A12})$$

509 **Acknowledgment**

510 Fundamental research of this paper was initiated by the BfG (German Federal Institute of Hydrology )  
511 with financial support. Special thanks are given to the Global Runoff Data Centre (GRDC) in Germany  
512 for offering the discharge data and the German Meteorological Service (DWD) for precipitation and  
513 temperature data. All the authors deeply appreciate all the reviewers for the efforts for examining and  
514 inspecting this work.

Formatted: No underline

515 **References**

- 516 Bárdossy, a., Pegram, G., 2009. Copula based multisite model for daily precipitation simulation. Hydrol.  
517 Earth Syst. Sci. Discuss. 6, 4485–4534. doi:10.5194/hessd-6-4485-2009
- 518 Bárdossy, A., 2006. Copula-based geostatistical models for groundwater quality parameters. Water Resour.  
519 Res. 42, W11416. doi:10.1029/2005WR004754
- 520 Bárdossy, A., Li, J., 2008. Geostatistical interpolation using copulas. Water Resour. Res. 44, W07412.  
521 doi:10.1029/2007WR006115
- 522 Bergström, S., 1976. Development and application of a conceptual runoff model for Scandinavian  
523 catchments, Bulletin Series A, A]: [Bulletin series. Department of Water Resources Engineering, Lund  
524 Institute of Technology, University of Lund.
- 525 Bergstrom, S., 1995. The HBV Model. Singh, V.P. (Ed.), Comput. Model. Watershed Hydrol. 443–476.
- 526 Box, G.E.P., Jenkins, G.M., 1976. Time series analysis: forecasting and control, revised ed. Holden-Day,  
527 San Francisco,USA.
- 528 Brahimi, B., Chebana, F., Necir, A., 2014. Copula representation of bivariate L-moments: a new  
529 estimation method for multiparameter two-dimensional copula models. Statistics (Ber). 1–25.
- 530 De Michele, C., Salvadori, G., 2003. A Generalized Pareto intensity-duration model of storm rainfall  
531 exploiting 2-Copulas. J. Geophys. Res. Atmos. 108, 4067. doi:10.1029/2002JD002534
- 532 Gao, P., Geissen, V., Ritsema, C., Mu, X.-M., Wang, F., 2012. Impact of climate change and  
533 anthropogenic activities on stream flow and sediment discharge in the Wei River basin, China. Hydrol.  
534 Earth Syst. Sci. Discuss. 9, 3933–3959. doi:10.5194/hessd-9-3933-2012
- 535 Grimaldi, S., 2004. Linear parametric models applied to daily hydrological series. J. Hydrol. Eng. 9, 383–  
536 391. doi:10.1061/(ASCE)1084-0699(2004)9:5(383)

Formatted: English (U.S.)

537 Huang, N.E., Shen, Z., Long, S.R., Wu, M.C., Shih, H.H., Zheng, Q., Yen, N.-C., Tung, C.C., Liu, H.H.,  
538 1998. The empirical mode decomposition and the Hilbert spectrum for nonlinear and non-stationary time  
539 series analysis. *Proc. R. Soc. London. Ser. A Math. Phys. Eng. Sci.* 454, 903–995.

540 Joe, H., 1997. *Multivariate models and multivariate dependence concepts*. Chapman&Hall, London.

541 Karlsson, I.B., Sonnenborg, T.O., Jensen, K.H., Refsgaard, J.C., 2014. Historical trends in precipitation  
542 and stream discharge at the Skjern River catchment, Denmark. *Hydrol. Earth Syst. Sci.* 18, 595–610.  
543 doi:10.5194/hess-18-595-2014

544 Lammersen, R., Engel, H., Van de Langemheen, W., Buiteveld, H., 2002. Impact of river training and  
545 retention measures on flood peaks along the Rhine. *J. Hydrol.* 267, 115–124. doi:10.1016/S0022-  
546 1694(02)00144-0

547 Li, J., 2010. *Application of copulas as a new geostatistical tool*. PhD Thesis. Nr. 187. University of  
548 Stuttgart, Germany

549 Nelsen, R.B., 2006. *An Introduction to Copulas*. Springer, New York. doi:10.1007/0-387-28678-0

550 Pettitt, A.N., 1979. A non-parametric approach to the change-point problem. *Appl. Stat.* 126–135.

551 Samaniego, L., Bárdossy, A., Kumar, R., 2010. Streamflow prediction in ungauged catchments using  
552 copula-based dissimilarity measures. *Water Resour. Res.* 46, W02506. doi:10.1029/2008WR007695

553 [Serfling, R., Xiao, P., 2007. A contribution to multivariate L-moments: L-comoment matrices. J. Multivar.  
554 Anal. 98, 1765–1781. doi:10.1016/j.jmva.2007.01.008](#)

555 Sharifdoost, M., Mahmoodi, S., Pasha, E., 2009. A statistical test for time reversibility of stationary finite  
556 state Markov chains. *Appl. Math. Sci.* 52, 2563–2574.

557 Siepe, A., 2006. *Dynamische Überflutungen am Oberrhein : Entwicklungs-Motor für die Auwald-Fauna.*  
558 *Stand* 149–158.

559 Singh, S.K., McMillan, H., Bárdossy, A., 2013. Use of the data depth function to differentiate between  
560 case of interpolation and extrapolation in hydrological model prediction. *J. Hydrol.* 477, 213–228.  
561 doi:10.1016/j.jhydrol.2012.11.034

562 Sklar, A., 1959. *Fonctions de répartition à n dimensions et leurs marges*, Publications de l’Institut de  
563 statistique de l’Université de Paris. Publications de l’Institut de Statistique de L’Université de Paris 8.

564 Sugimoto, T., 2014. *Copula based stochastic analysis of discharge time series*. PhD Thesis. Nr. 232.  
565 University of Stuttgart, Germany

566 Wu, C.S., Yang, S.L., Lei, Y.P., 2012. Quantifying the anthropogenic and climatic impacts on water  
567 discharge and sediment load in the Pearl River (Zhujiang), China (1954–2009). *J. Hydrol.* 452–453, 190–  
568 204. doi:10.1016/j.jhydrol.2012.05.064

Formatted: English (U.S.)

Formatted: English (U.S.)

570

571 Table 1 Variance and copula variance calculated for 4 discharge time series

572  
573

	ANDE	COCH	MAXA	PLOC
<i>Var</i>	1.79	2.24	1.75	2.72
<i>Var<sub>cop</sub></i> [ $\times 10^{-5}$ ]	3.01	1.64	5.39	1.27

574

575 Table 2 Covariance, correlation, copula covariance and copula correlation between 4 discharge data

576 (AN:Andernach, CO:Cochem, MA:Maxau, PL:Plochingen)

577  
578

	AN-CO	AN-MA	AN-PL	CO-MA	CO-PL	MA-PL
<i>Cov</i>	1.68	1.60	1.33	1.38	1.31	1.41
<i>Cor</i>	0.84	0.90	0.60	0.70	0.53	0.64
<i>Cov<sub>cop</sub></i> [ $\times 10^{-6}$ ]	4.90	3.40	3.39	7.16	9.90	5.47
<i>Cor<sub>cop</sub></i>	0.60	0.77	0.46	0.71	0.60	0.59

579

580 Table 3 Variance and copula variance calculated for API time series of 4 regions in the Baden-

581 Württemberg state of Germany

582  
583

	C	SW	NW	NE
<i>Var</i>	1.70	1.66	1.72	1.78
<i>Var<sub>cop</sub></i> [ $\times 10^{-6}$ ]	3.00	4.02	3.35	3.21

584

585

586 Table 4 Covariance, correlation, copula covariance and copula correlation between API time series from 4

587 regions in the Baden-Württemberg state of Germany

588  
589

	C-SW	C-NW	C-NE	SW-NW	SW-NE	NW-NE
<i>Cov</i>	1.35	1.33	1.44	1.25	1.41	1.42
<i>Cor</i>	0.80	0.77	0.84	0.74	0.84	0.83
<i>Cov<sub>cop</sub></i> [ $\times 10^{-7}$ ]	1.46	1.16	8.94	4.42	1.11	8.80
<i>Cor<sub>cop</sub></i>	0.36	0.29	0.29	0.09	0.26	0.24

590

Figure Captions

Figure 1 Locations of 7 discharge gauging stations in the Upper Rhine Region

Figure 2 Visualization of the functions which displays the contribution of a realization of  $(U_t, U_{t+k})$  to *assymetry1* (left) and *assymetry2* (right)

Figure 3 Sketch of the transformation from sample hydrograph (left) to empirical copula (right): Scatterplot of ranks are calculated from two values separated by time lag  $k = 1$  [days] in a discharge time series of Andernach where *rank correlation* = 0.9870,  $A_1(k = 1) = -0.0002398$  and  $A_2(k = 1) = -0.00011037$ . The possible combinations of high and low values, which has large impacts on asymmetry, are numbered (1) low to high, (2) high to high (3) high to low (4) low to low. Negative contribution to *assymetry2* is drawn with red circle, positive contribution with blue circle.

Figure 4 Annual cycle of mean discharge after smoothing (left) and annual cycle of standard deviation after smoothing (right)

Figure 5 Discharge time series between 1950 and 1955 before applying normalization (upper left) and after applying normalization (upper right). The variation of *assymetry2* function calculated for entire time series before applying normalization (bottom left) and after applying normalization (bottom right) with 90% confidence intervals (grey) calculated for 100 realizations of Gaussian process (dashed line is  $A_2(k)$  calculated for one of the realization of Gaussian process ).

Figure 6 Relation between Asymmetry and catchment characteristics: minimum of *assymetry2* of discharge and catchment area (top), lag at minimum of *assymetry2* of discharge and catchment area (middle), minimum of *assymetry2* of discharge and lag at minimum of *assymetry2* of discharge (bottom)

Figure 7 Temporal change of minimum of *assymetry2* for 7 discharge records and confidence intervals calculated from the Gaussian process (90% confidence interval with grey color and 60% confidence interval with dark grey color) and one of its realizations (dashed line)

Figure 8 Moving average and standard deviation of the 7 daily discharge records for the window size  $w = 3000$

Figure 9 Annual minimum and mean of aggregated daily temperature in the Baden-Württemberg state of Germany

Figure 10 Copula distances of discharge time series in moving time window: moving variance (top), distance type1 (middle) and distance type2 (bottom) with 80% confidence interval of Gaussian process and one of its realization (dashed line)

Figure 11 Copula distances of discharge time series in moving time window: moving covariance (top), moving correlation (second), distance type3 (third) and distance type4 (bottom)

Figure 12 Locations of the precipitation gauge stations within the Baden-Württemberg (Germany) indicated by coloured circles. Upper Neckar catchment is drawn with green area and the location of gauging station is drawn with a square

627 Figure 13 Copula distances of API time series in moving time window: moving variance (top), copula  
628 distance type1 (middle) and copula distance type2 (bottom) where ‘C’ denotes central, ‘SW’ denotes  
629 southwest, ‘NW’ denotes northwest and ‘NE’ denotes northeast part of Baden-Württemberg State of  
630 Germany respectively with 80% confidence interval of Gaussian process and one of its realization (dashed  
631 line).

632 Figure 14 Copula distances of API time series in moving time window: moving covariance (top), moving  
633 correlation (second), distance type3 (third) and distance type4 (bottom)

634 Figure 15 Copula distance type3 (top) and type4 (bottom) between 4 discharge and 1 API time series  
635 which is aggregated for all the daily precipitations depicted in Figure 12

636 Figure 16 Copula asymmetry and copula distances for 30 simulated and one observed discharge time series  
637 at Plochingen between 1965 and 2000: minimum of asymmetry2 for the time lag  $k = 2$  [days] (top), copula  
638 distance type1 (middle), copula distance type2 (bottom)

639

640

641

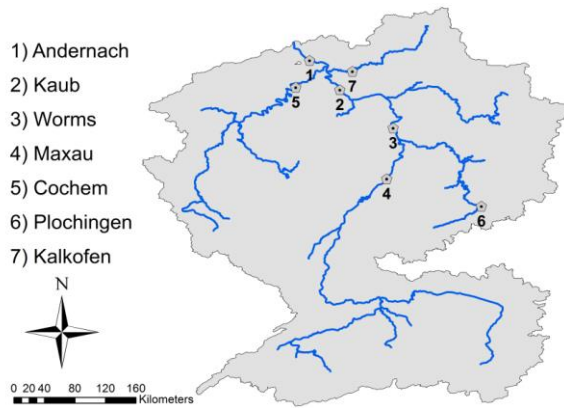


Figure 1 Locations of 7 discharge gauging stations in the Upper Rhine Region

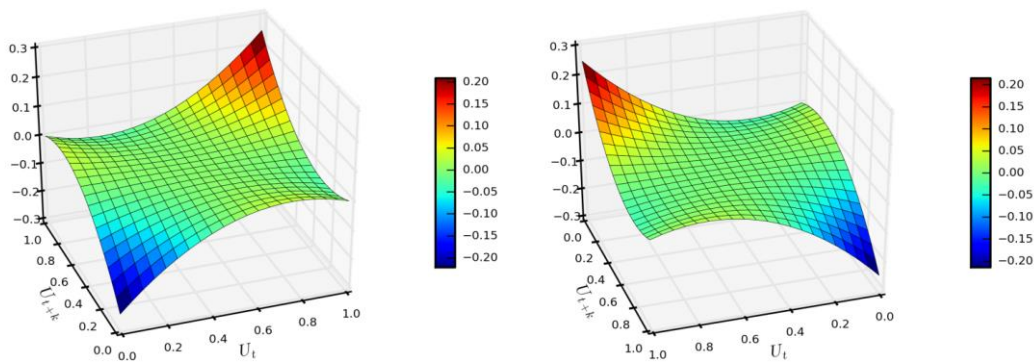
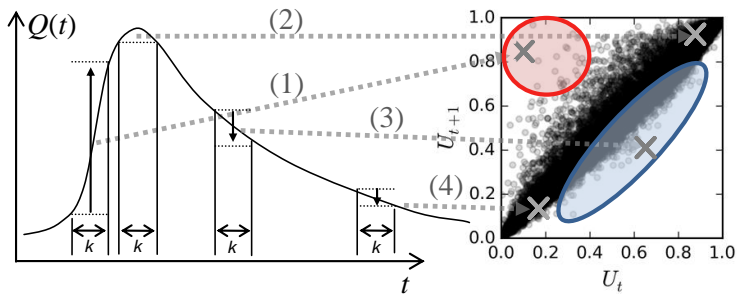


Figure 2 Visualization of the functions which displays the contribution of a realization of  $(U_t, U_{t+k})$  to *assymetry1* (left) and *assymetry2* (right)



Formatted: Centered

Figure 3 Sketch of the transformation from sample hydrograph (left) to empirical copula (right): Scatterplot of ranks are calculated from two values separated by time lag  $k = 1$  [days] in a discharge time series of Andernach where rank correlation = 0.9870,  $A_1(k = 1) = -0.0002398$  and  $A_2(k = 1) = -0.00011037$ . The possible combinations of high and low values, which has large impacts on asymmetry, are numbered (1) low to high, (2) high to high (3) high to low (4) low to low. Negative contribution to asymmetry2 is drawn with red circle, positive contribution with blue circle.

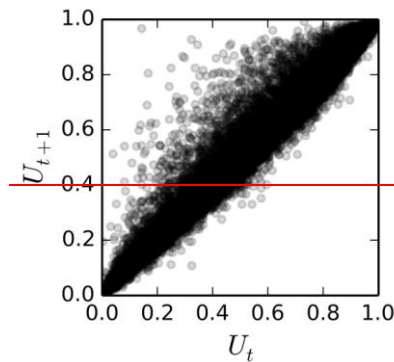


Figure 3 Scatterplot of ranks calculated from two values separated by time lag  $k = 1$  [days] in a discharge time series of Andernach where rank correlation = 0.9870,  $A_1(k = 1) = -0.0002398$  and  $A_2(k = 1) = -0.00011037$

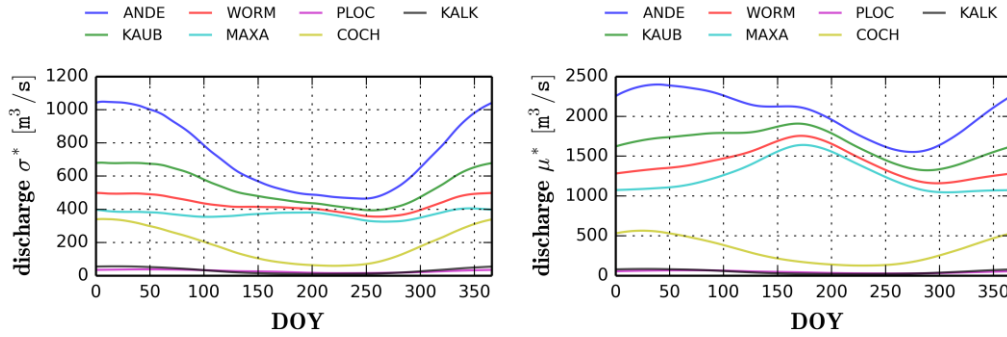


Figure 4 Annual cycle of mean discharge after smoothing (left) and annual cycle of standard deviation after smoothing (right)

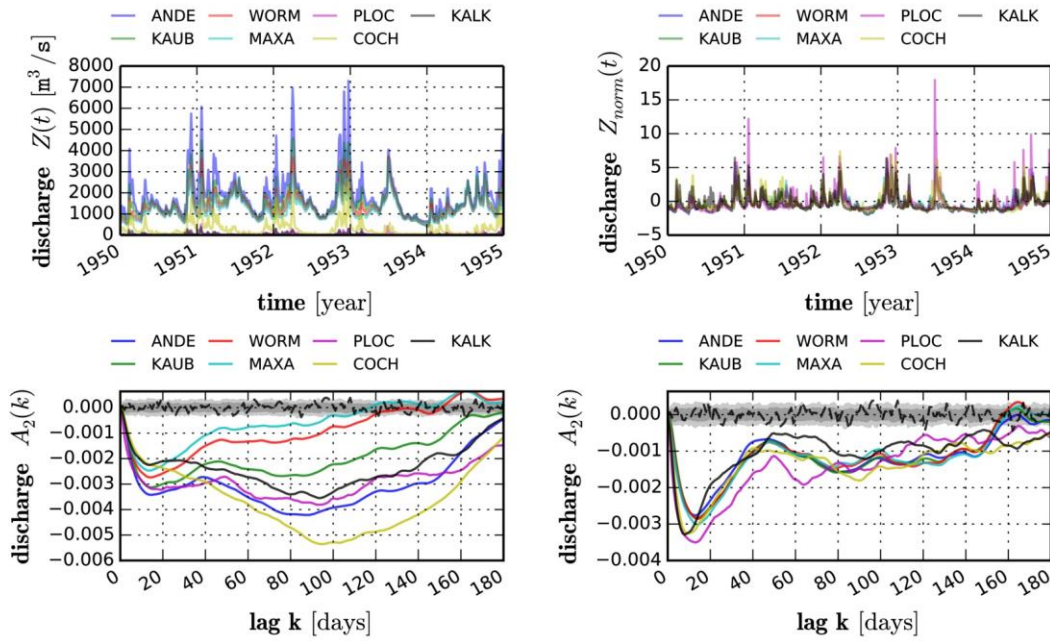
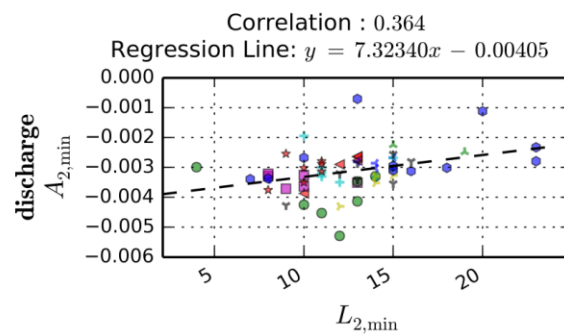
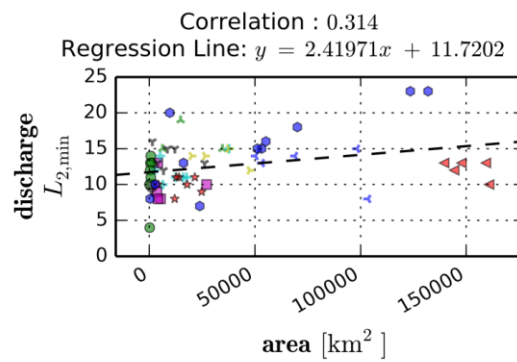
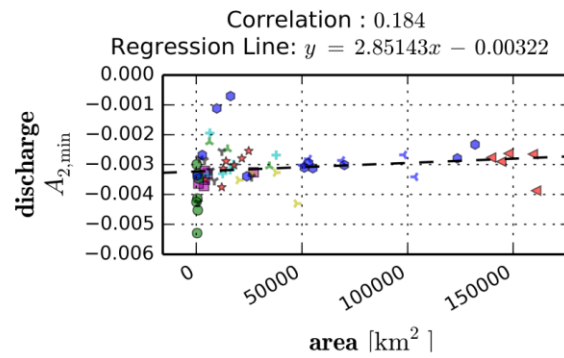
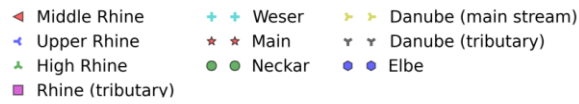


Figure 5 Discharge time series between 1950 and 1955 before applying normalization (upper left) and after applying normalization (upper right). The variation of asymmetry2 function calculated for entire time series before applying normalization (bottom left) and after applying normalization (bottom right) with 90% confidence intervals (grey) calculated for 100 realizations of Gaussian process (dashed line is  $A_2(k)$  calculated for one of the realization of Gaussian process ).



669

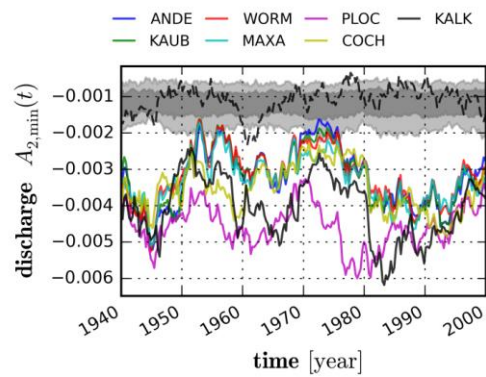
670 Figure 6 Relation between Asymmetry and catchment characteristics: minimum of asymmetry2 of

671 discharge and catchment area (top), lag at minimum of asymmetry2 of discharge and catchment area

672 (middle), minimum of asymmetry2 of discharge and lag at minimum of asymmetry2 of discharge (bottom)

673

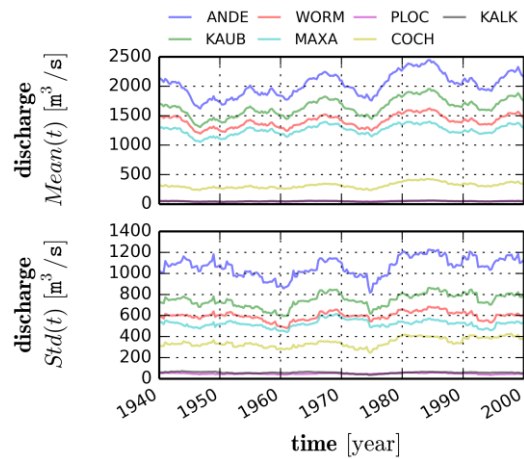
674



675

676 Figure 7 Temporal change of minimum of asymmetry2 for 7 discharge records and confidence intervals  
677 calculated from the Gaussian process (90% confidence interval with grey color and 60% confidence  
678 interval with dark grey color) and one of its realizations (dashed line)

679



680

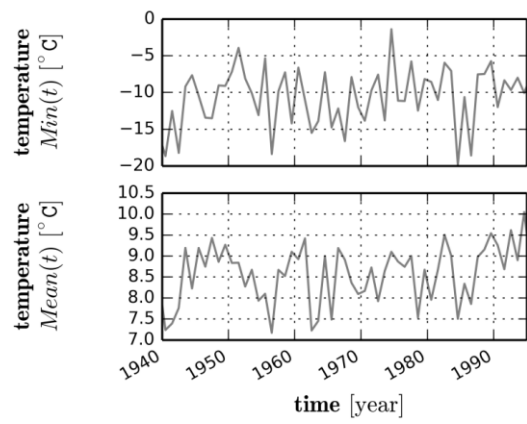
681 Figure 8 Moving average and standard deviation of the 7 daily discharge records for the window size  $w =$

682 3000

683

684

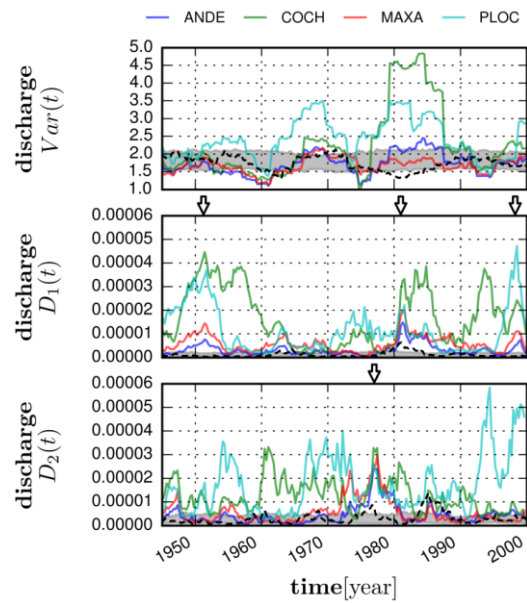
685



686

687 Figure 9 Annual minimum and mean of aggregated daily temperature in the Baden-Württemberg state of

688 Germany



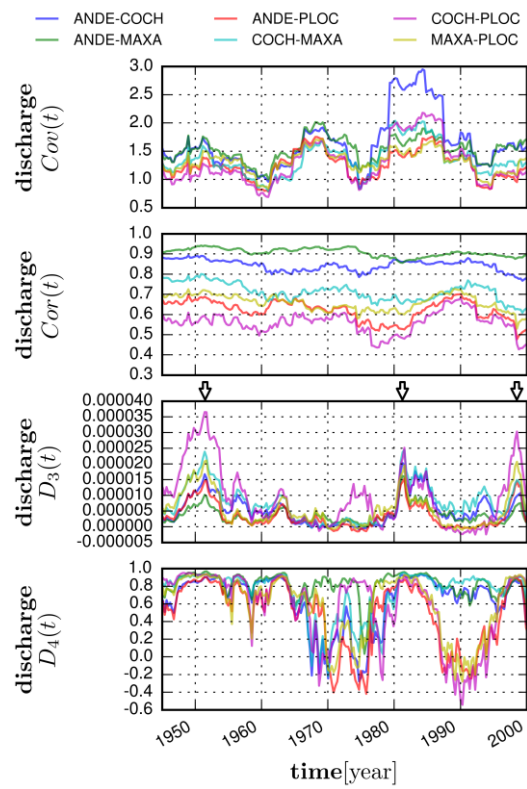
689

690 Figure 10 Copula distances of discharge time series in moving time window: moving variance (top),

691 distance type1 (middle) and distance type2 (bottom) with 80% confidence interval of Gaussian process and

692 one of its realization (dashed line)

693



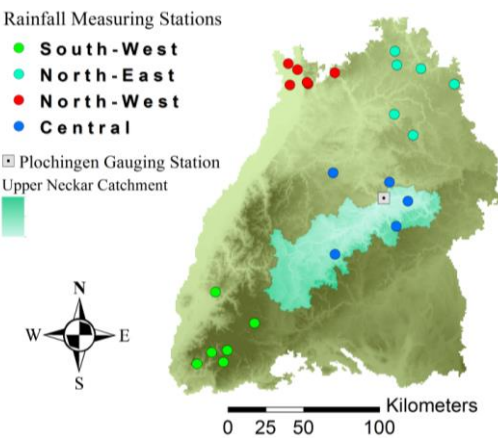
694

695 Figure 11 Copula distances of discharge time series in moving time window: moving covariance (top),

696 moving correlation (second), distance type3 (third) and distance type4 (bottom)

697

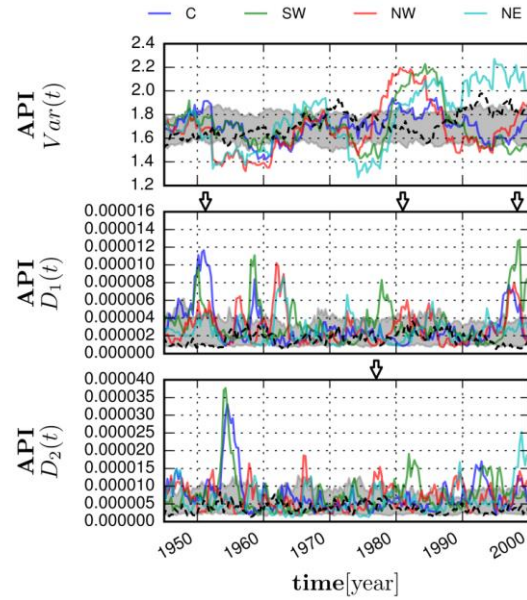
698



699

700 Figure 12 Locations of the precipitation gauge stations within the Baden-Württemberg (Germany)  
701 indicated by coloured circles. Upper Neckar catchment is drawn with green area and the location of  
702 gauging station is drawn with a square

703



704

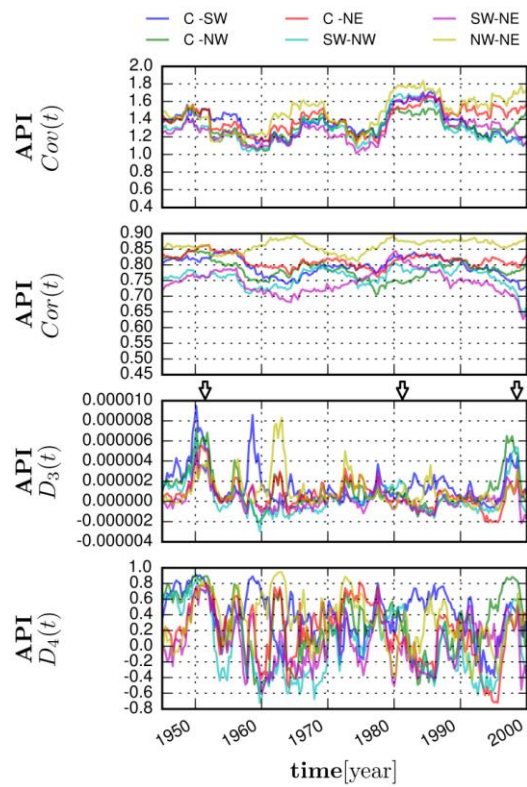
705 Figure 13 Copula distances of API time series in moving time window: moving variance (top), copula  
 706 distance type1 (middle) and copula distance type2 (bottom) where ‘C’ denotes central, ‘SW’ denotes  
 707 southwest, ‘NW’ denotes northwest and ‘NE’ denotes northeast part of Baden-Württemberg State of  
 708 Germany respectively with 80% confidence interval of Gaussian process and one of its realization (dashed  
 709 line).

710

711

712

713

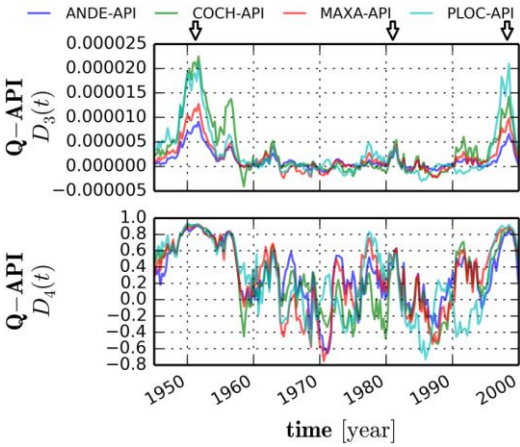


714

715 Figure 14 Copula distances of API time series in moving time window: moving covariance (top), moving  
716 correlation (second), distance type3 (third) and distance type4 (bottom)

717

718

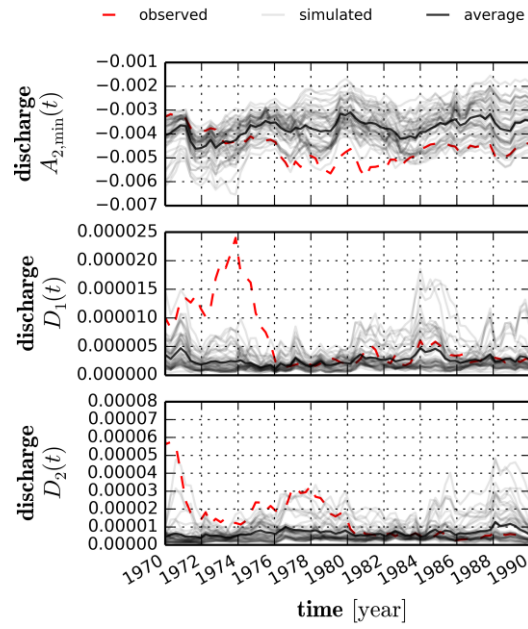


719

720 Figure 15 Copula distance type3 (top) and type4 (bottom) between 4 discharge and 1 API time series

721 which is aggregated for all the daily precipitations depicted in [Figure 12](#)~~Figure 12~~

722



723

724 Figure 16 Copula asymmetry and copula distances for 30 simulated and one observed discharge time series  
 725 at Plochingen between 1965 and 2000: minimum of asymmetry2 for the time lag  $k = 2$  [days] (top), copula  
 726 distance type1 (middle), copula distance type2 (bottom)

727

728

729

730